

Iterative Convolution Calculations of Particle Scattering Functions for Self-Avoiding Polymer Systems

Clive A. Croxton

Department of Mathematics, University of Newcastle, NSW 2308, Australia.
Received December 29, 1987

ABSTRACT: Scattering functions in the form of Kratky plots are determined on the basis of the iterative convolution (IC) approximation for a wide variety of polymer geometries incorporating excluded-volume effects. The Kratky plots are in good to excellent agreement with Monte Carlo estimates over the entire range of the scattering vector and appear to represent a substantial improvement upon existing limiting and asymptotic estimates based upon Gaussian statistics and perturbative departures therefrom. The structures of the Kratky plots are analyzed in terms of the component weighting functions W_i associated with scattering from centers $i, i+\nu$ ($\nu = 0, \dots, N-1$). The IC technique appears to provide a unified description of polymer scattering and structure for all molecular geometries considered here.

Introduction

The description of scattering from isolated polymer systems of various geometries appears to be largely restricted to Gaussian-based analyses in which the excluded-volume features of the sequence are totally neglected. Moreover, such expressions for the scattering function generally relate to limiting ranges of the scattering vector and apply to sequences of infinite length. We present here an iterative convolution (IC) description of coherent scattering over the entire range of scattering angle for finite heterogeneous sequences which may incorporate specific skeletal features, including excluded-volume effects and nonlinear geometries. We compare our predictions with Monte Carlo simulations wherever possible and find that the agreement of the IC determinations with the MC data ranges from good to excellent over the entire scattering domain for a wide variety of macromolecular geometries. First, however, we briefly review the Gaussian treatments of polymer scattering.

The ratio of the coherent scattering intensity $I(Q)$ to $I(0)$ at scattering vector magnitude $Q = (4\pi/\lambda) \sin(\theta/2)$ is given by the relation

$$I(Q)/I(0) = P(Q)S(Q) \quad (1)$$

where λ is the wavelength of the scattered radiation within the system and $P(Q)$ is the particle scattering function relating to intramolecular structure, while $S(Q)$, the scattering factor, relates to interparticle distributions. For sufficiently dilute systems $S(Q)$ may be set to unity, whereupon

$$I(Q)/I(0) = P(Q) \quad (2)$$

Although both $P(Q)$ and $S(Q)$ arise as Fourier transforms of the interparticle spatial distributions on self and distinct molecules, respectively, we restrict the present discussion to dilute systems and consider the particle scattering function $P(Q)$ only. For a system of N identical point scattering centers

$$P(Q) = \frac{1}{N^2} \sum_i \sum_j \langle \exp(2\pi \mathbf{Q} \cdot \mathbf{r}_{ij}) \rangle \quad (3)$$

where \mathbf{r}_{ij} is the separation of centers i, j within the molecule. Averaging over all orientations eq 3 becomes

$$P(Q) = \frac{1}{N^2} \sum_i \sum_j \left\langle \frac{\sin(Qr_{ij})}{Qr_{ij}} \right\rangle \quad (4)$$

where $\langle \dots \rangle$ represents the spatial average over the scalar separation r_{ij} . If the scattering centers i, j are not identical but have contrast factors g_i, g_j , respectively, then eq 4 generalizes to become

$$P(Q) = \frac{\sum_i \sum_j g_i g_j \left\langle \frac{\sin(Qr_{ij})}{Qr_{ij}} \right\rangle}{\sum_i \sum_j g_i g_j} \quad (5)$$

Now, the spatial averages in eq 4 and 5 are nothing other than the Fourier transforms of $Z(r_{ij}|N)$, the normalized spatial probability distribution function between centers i and j in the N -mer, whereupon for a system of identical point scattering centers:

$$P(Q) = \frac{1}{N^2} \sum_i \sum_j \tilde{Z}(ij|N) \quad (4a)$$

where \sim denotes the Fourier transform. Of course, the determination of $Z(r_{ij}|N)$ represents one of the fundamental objectives of modern polymer theory; in general, calculations of $P(Q)$ have been restricted to systems unperturbed by excluded-volume effects¹ or have used Monte Carlo techniques to establish the spatial averages in the equations above.^{2,3,7} In the context of the present paper it is particularly convenient to review briefly the principal descriptions of the scattering function as they relate to chains unperturbed by excluded-volume effects and then to extend the discussion to include their perturbed counterparts.

Provided we restrict ourselves to sufficiently small Q such that we may expand $\sin(Qr_{ij})$ to first order (the Guinier region), eq 4 assumes the form

$$P(Q) = 1 - \frac{Q^2 \langle S_N^2 \rangle}{3} + \dots \quad (6)$$

where $\langle S_N^2 \rangle$ is the mean-square radius of gyration of the molecule. It is generally more convenient to present the scattering distributions in the form of a Kratky plot in which $P(Q)NQ^2$ is plotted against Q , and the qualitative form of the Guinier region is shown schematically in Figure 1.

Unperturbed Systems

If excluded-volume effects within a system of identical point scatterers are totally neglected, (i) the $Z(ij|N)$ assume the form of Gaussian probability distributions provided $|i-j| \gg 1$ and (ii) $\langle R_{ij}^2 \rangle = l_0|i-j|$ where l_0 is the bond length. We shall refer to these as the "Gaussian assumptions" throughout the rest of this paper. On this basis Debye⁴ derived the following expression for the particle scattering function of a linear N -mer in Kratky form:

$$P(Q)NQ^2 = 2 \frac{NQ^2}{x^2} (x - 1 + e^{-x}) \quad (7)$$

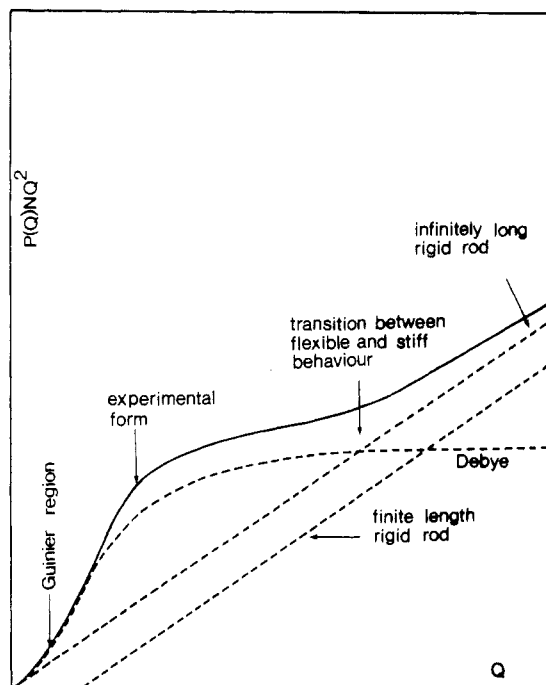


Figure 1. Schematic form of the Kratky representation of the scattering function $P(Q)NQ^2$ vs Q for a linear sequence in various limiting approximations.

where $x = Q^2 \langle S_N^2 \rangle = Q^2 l_0^2 N(N+2)/6(N+1)$ for linear Gaussian chains. At small Q , eq 7 reduces to Guinier form and evidently provides a qualitative description of the gross geometrical features of the macromolecule. However, eq 7 cannot be expected to adequately describe the high- Q region of realistic systems since this relates directly to scattering on the monomer scale at which excluded-volume and stereochemical features of the system become important, but are of course neglected in the Gaussian approximation. Moreover, this short-range structure extends into the high- Q region of the Kratky curve but remains unresolved in the Debye representation. At intermediate to large $Q \langle S_N^2 \rangle$ the Kratky function ($P(Q)NQ^2$) based on the Debye approximation (eq 7) develops a plateau region characteristic of unperturbed systems and provides a means of qualitative assessment of the configurational processes which determine the form of the scattering function for realistic systems. The qualitative form of the Debye scattering function is presented as a Kratky plot in Figure 1. It should be emphasised from the outset, however, that the development of a plateau region in the Kratky curve for realistic systems does not necessarily imply Gaussian behavior, as we shall see.

A rotational isomeric state model (RISM) was used by Flory et al.⁵ in conjunction with realistic molecular parameters to generate the even moments $\langle r_{ij}^{2m} \rangle$ in terms of which it is possible to form the Nagai series expansion of $\langle \sin(Qr_{ij})/Qr_{ij} \rangle$:

$$\left\langle \frac{\sin Qr_{ij}}{Qr_{ij}} \right\rangle = \exp \left[\frac{-Q^2 \langle r_{ij}^2 \rangle}{6} \right] \sum_{m=0}^{\infty} g_{2m} Q^{2m}$$

where $g_0 = 1$, $g_2 = 0$, and

$$g_{2m} = \sum_{k=0}^{m-2} \frac{(-1)^{m-k} \langle r_{ij}^{2k} \rangle \langle r_{ij}^{2(m-k)} \rangle}{(3!)^k k! [2(m-k) + 1]!} - \frac{(m-1) \langle r_{ij}^2 \rangle^m}{(3!)^m m!} \quad (8)$$

for $m \geq 2$.

In fact, convergence of the Nagai series is known to be slow and oscillatory,^{7,9} and accordingly moments of high order need to be formed. Some simplification is achieved

by replacing $\langle r_{ij}^{2m} \rangle$ by $\langle r_n^{2m} \rangle$ where $n = |i - j|$, although this denies the dependence of a given moment upon the location of the subset n within the sequence. The higher order moments may be calculated by generator matrix techniques,⁸ and although there have been some subsequent attempts⁶ to apply the method to systems embodying excluded-volume effects, this approach of Flory et al. may only be consistently applied to unperturbed systems.

The persistence chain model, while taking no account of excluded volume, nevertheless recognizes the restricted flexibility arising from a mean or fixed valence angle α between adjacent bonds. In the case of fixed valence angles, chain flexibility derives solely from RISM-like rotations about the axis of the bond. A stiffness parameter $s = L/b$ is introduced where L is the contour length of the sequence and

$$b = l_0 \frac{1 + \cos \langle \alpha \rangle}{1 - \cos \langle \alpha \rangle} \quad (9)$$

where l_0 is the bond length. For perfectly flexible Gaussian chains $\langle \alpha \rangle = \pi/2$ and $b = l_0$.

As $\langle \alpha \rangle$ decreases so the sequence stiffens, becoming a rigid rod of length L at $\alpha = 0$. Evidently the persistence chain model is capable of describing the full range of chain flexibilities ranging from the Gaussian coil to a rigid rod. An analysis of the principal geometrical features of a continuous persistence chain (wormlike model) has been presented on the basis that both $\langle \alpha \rangle$ and $l_0 \rightarrow 0$, while $s = L/b$ remains constant. The associated Kratky function at small to intermediate Q has been determined by Sharp and Bloomfield²³ to be

$$P(Q)NQ^2 = 2 \frac{NQ^2(e^{-x} + x - 1)}{x^2} + bQ^2 \left[\frac{4}{15} + \frac{7}{15x} - \left(\frac{11}{15} + \frac{7}{15x} \right) \right] \quad (10)$$

where $x = Q^2 Lb/6$.

At small s , corresponding to stiff chains, the large Q scattering assumes the form appropriate to the structure factor of a thin rod of length L which has been determined by Neugebauer¹⁰ to be of the form

$$P(Q)NQ^2 = \frac{N\pi Q}{L} - \frac{2N}{L^2} \quad (11)$$

which in a Kratky plot assumes the form of a line of slope $N\pi/L$ having the intercept $-2N/L^2$ at $Q = 0$. The more flexible the chain the higher is the value of Q at which rodlike scattering is appropriate. des Cloiseaux¹⁴ has, in fact, determined $P(Q)$ for the persistence chain model at all Q in the limit $L \rightarrow \infty$. The limiting form of the Kratky function as $Q \rightarrow 0$ is then

$$P(Q)NQ^2 = \frac{12}{b} + \frac{4bQ^2}{15} \quad (12)$$

which follows from eq 1, while for large Q

$$P(Q)NQ^2 = \pi Q + 4/3b \quad (13)$$

These various features of the scattering curve are presented qualitatively in the form of a Kratky plot (Figure 1), from which we observe that the point P identifies the spatial scale over which the sequence can be described as having made the transition from flexibility to stiffness. Clearly the transition will occur at higher Q with increasing chain flexibility.

While the above results relate essentially to unperturbed linear systems, their qualitative form will prove useful in assessing the role of excluded volume in realistic sequences for which no analytic descriptions have yet been deter-

mined, although Monte Carlo simulations of such systems have been frequently reported.

The corresponding Kratky function for uniform unperturbed star polymers having f identical branches of n monomers per branch has been given by Benoit:¹¹

$$P(Q)NQ^2 = \frac{2NQ^2}{x^2} \left[\frac{f}{2}(f-1)e^{-2x/f} - f(f-2)e^{-x/f} + x + \frac{f}{2}(f-3) \right] \quad (14)$$

where $x = Q^2 \langle S_N^2 \rangle = Q^2 f^2 (3f-2) l_0^2 N(N+2)/6(N+1)$ for uniform Gaussian stars and $N = nf + 1$.

In the Guinier region the curve would be expected to reflect the Zimm-Stockmayer result¹³ $\langle S_N^2 \rangle_{\text{star}} / \langle S_N^2 \rangle_{\text{linear}} = (3f-2)/f^2$ for star and linear molecules having the same number of identical statistical units. This function also develops a characteristic plateau at intermediate to large Q , as does the Kratky curve for unperturbed rings. However, in the case of rings, Casassa and Burchard and Schmidt¹² assumed that the segmental pair distribution function differs from a Gaussian chain only in that the first and last segments are joined together, in which case the pair distribution function is represented as a convolution of two Gaussian subchains connecting any pair of segments. This yields the scattering function

$$P(Q) = (2/x)^{1/2} D((x/2)^{1/2}) \quad (15)$$

where $x = Q^2 \langle S_N^2 \rangle$ and D is the Dawson integral.¹⁶ The above expression predicts a maximum in the Kratky plot, followed by the usual Debye plateau at larger Q . While of the same qualitative form in the Guinier region, the Gaussian rings nevertheless reflect the Zimm-Stockmayer result¹³ $\langle S_N^2 \rangle_{\text{ring}} / \langle S_N^2 \rangle_{\text{linear}} = 1/2$ for molecules of the same molecular weight.

In the absence of an adequate prescriptive basis for $Z(ij|N)$, many investigators have utilized Monte Carlo techniques for the estimation of $\langle \sin(Qr_{ij})/Qr_{ij} \rangle$,⁹ and while it is not appropriate to review them here, the simulations generally relate to linear sequences unperturbed by excluded-volume effects, although features of the RISM model are frequently incorporated. A recent example of such a procedure is the Monte Carlo RISM determinations of Edwards et al.² in which Metropolis samplings for unperturbed polymethylene, poly(oxyethylene), and poly(dimethylsiloxane) chains up to 150 skeletal bonds are determined by using established molecular parameters for the t, g^+ and g^- rotational states. Particle scattering functions were determined on the assumption that the scattering centers are located on or near the skeletal atoms, and we shall adopt the same approximation in our iterative convolution (IC) calculations. Although we are not attempting to model specific systems, unlike Edwards et al., it is appropriate to mention that Yoon and Flory,³ for example, found that for short polymethylene chains small-angle neutron scattering data at intermediate Q could only be reproduced exactly when the double sums in eq 4 extended over every pair of protons in the chain. Nevertheless, Edwards et al. find that the single-center approximation is highly satisfactory and we adopt the same point scattering approximation, although in the present IC calculations the results are no longer compromised by the neglect of excluded-volume effects.

Perturbed Systems

The incorporation of excluded volume into the configurational statistics of polymeric systems of various geometries has been modeled in a variety of ways ranging from lattice-based and renormalization group analyses to iter-

ative convolution treatments. Invariably, the principal configurational properties such as mean-square end-to-end length and mean-square radius of gyration of perturbed systems exhibit a limiting dependence upon chain length of the form $\sim (N-1)^{(1+\epsilon)}$. There appears to be general agreement that with increasing chain length $\epsilon \rightarrow 0.2$, while for $\epsilon = 0$ we recover the unperturbed results appropriate to Θ conditions. A generalization of the Gaussian spatial probability distribution to include the perturbed case has been obtained by Fisher¹⁵ in the limit $|i-j| \rightarrow \infty$:

$$Z(ij) = Cr_{ij}^s \exp[-(r_{ij}/\sigma)^t] \quad (16)$$

where

$$C = \frac{t}{\sigma^{s+1} \Gamma\left(\frac{s+1}{t}\right)} \quad \text{and} \quad \sigma^2 = \frac{\langle r_{ij}^2 \rangle \Gamma\left(\frac{s+1}{t}\right)}{\Gamma\left(\frac{s+3}{t}\right)}$$

and where $t = 2/(1-\epsilon)$. With $\epsilon = 0$ and $s = t = 2$ we recover the Gaussian distribution. The best fit with experimental data appears to occur for $\epsilon = 0.2$, $s = 2.8$, and $t = 2.5$, suggesting a sharper distribution than the Gaussian with a reduction in the probability of short-range separations,¹ in accord with the known form of $Z(ij)$ for excluded-volume systems determined on the basis of Monte Carlo estimates. Such a parametric fit is not entirely satisfactory, however, and a priori determinations must remain the primary objective of any unified theory of polymer structure and scattering. Nevertheless, such a distribution yields a Kratky curve of the form

$$P(Q)NQ^2 \sim Q^{2\epsilon} \quad (17)$$

for intermediate to large Q , and we recover the Debye plateau in the Gaussian limit, $\epsilon = 0$.

Linear Polymers

It is apparent from the preceding discussion that no unified description of polymer configuration and scattering, particularly for systems perturbed by excluded-volume effects, has yet been presented, although limiting relationships over restricted ranges of Q for variants of the Gaussian coil are available. In the absence of an adequate basis for the prescription of $\langle \sin(Qr_{ij})/Qr_{ij} \rangle$, a number of workers have adopted Monte Carlo techniques for the estimate of $\langle \dots \rangle$, basing their simulations on the RISM representation in which excluded volume is neglected, but a number of experimental characteristics such as bond angles and lengths and population of the various rotational states are incorporated.

The iterative convolution (IC) technique, which has been successfully applied to the description of the configurational properties of a wide variety of polymer systems,²⁰ relates the spatial probability distribution $Z(ij|N)$ between statistical elements ij within the N -mer to the central pair interaction $\Phi(r_{ij})$ operating between them. While it is not appropriate to review the IC technique here, but instead to refer the reader elsewhere,²¹ it is nevertheless useful to present the basic integral relation between the complete set of distributions $Z(ij|N)$ developed within the sequence and the interaction matrix $[\Phi]$:

$$Z(ij|N) = H(ij)\Pi' \int Z(ik|N)Z(kj|N) dk \quad (18)$$

where $H(ij) = \exp(-\Phi(r_{ij})/kT)$ and Π' represents the geometric mean of all convolution integrals mediated through segment $k \neq i, j$ and weighted by $(|i-k||k-j|)^{-1}$. This weighting function is introduced to reflect the differential contribution to the mean Π' arising from widely separated elements ij with respect to those whose contour separation

is much closer and whose contribution to the correlation mediated through segment k is likely to be more significant. This equation may be readily cast into iterative form

$$Z(ij|N) = H(ij) \int H(ik) \Pi' \int Z(il|N) Z(lk|N) dl \times \\ H(kj) \Pi' \int Z(km|N) Z(mj|N) dm dk \quad (19)$$

whereupon the convolution integrals may be readily evaluated by fast Fourier transform techniques (FFT). Now, the FFT's arising in the evaluation of these integrals are nothing other than the desired quantities $\langle \sin Qr_{ij}/Qr_{ij} \rangle$, and once the system of coupled integral equations has converged we have direct access to the scattering function defined in eq 4a. Indeed, it is clear that the solution of eq 19 is determined in terms of the pair scattering functions and $P(Q)$ arises almost as a byproduct in the IC technique. Experimental determinations based on small-angle optical, X-ray, and neutron scattering techniques are generally restricted to the region $Q \leq 0.5(\sigma^{-1})$, where σ is the segment diameter, beyond which incoherent scattering dominates. Here, however, we determine the scattering functions over the range $0 < Q < 32(\sigma^{-1})$, beyond which $P(Q)$ is essentially zero. Invariably we find that for $Q \geq 1(\sigma^{-1})$ the IC and MC determinations are graphically indistinguishable, and we therefore assert that we are able to determine the scattering function over the entire range of the scattering vector Q .

The incorporation of contrast factors is readily achieved in forming the double sum in eq 5, although a much more powerful approach is to form restricted sums over the $\langle \dots \rangle_{ij}$ in eq 4a, thereby specifically identifying those scattering contributions responsible for a particular feature of $P(Q)$. This we do below. It is also clear that the IC technique yields the scattering function over the entire range of Q and as such may be considered as a unified theory of structure and scattering from polymeric systems.

Although any set of well-behaved central pair interactions may be specified in $[\Phi]$, we restrict ourselves in this paper to perfectly flexible systems of hard-sphere sequences since the consideration of more exotic interactions would seem inappropriate when perturbation of chains by excluded-volume processes has not yet been properly incorporated. Moreover, the hard-sphere model is representative of a wide range of realistic systems and represents a convenient model for the Monte Carlo determination of the scattering functions with which we compare most of our IC calculations. In the Monte Carlo simulations we generate linear hard-sphere sequences in three dimensions, the chain being extended by the addition of a subsequent segment uniformly distributed over the surface of its predecessor until a geometric violation occurs. The violating segment is withdrawn, and the configurational statistics of the preceding "successful" configuration accrued. Data sets averaged over at least 2000 successful configurations at each chain length were established: the 95% confidence limits on the Monte Carlo scattering curves presented in this paper are graphically imperceptible, and the data appear as a continuous curve.

In Figure 2 we compare the Kratky plots for a perfectly flexible linear sequence of $N = 20$ hard-sphere segments of unit diameter determined on the basis of the IC and MC techniques. It is, perhaps, appropriate to point out that the scattering curve develops very little with increasing chain length beyond $N \sim 10$, and the $N = 20$ Kratky plot is likely to closely resemble the curves for substantially longer sequences. This is so because scattering at intermediate to large Q , which accounts for the majority of the function, relates to distances less than or equal to the correlation range of the monomers and the asymptotic

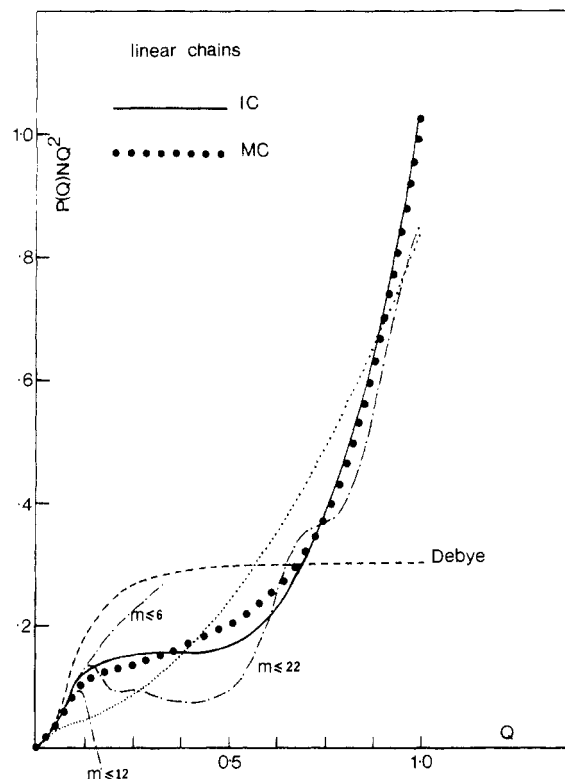


Figure 2. Kratky plots for a perfectly flexible hard-sphere linear sequence of $N = 20$ monomers on the basis of the IC approximation and other approximate analyses: (---) Nagai series expansions terminated at the m -th moment; (···) persistence chain representation ($b = 3$). The Monte Carlo data for a linear hard sphere sequence of 20 monomers is also shown.

form for $N \gg 1$ appears to be rapidly established. Here, the Kratky function is determined over the range $0 < Q < 32(\sigma^{-1})$ for both the MC and IC analyses and for all polymer geometries discussed in this paper. Beyond ($Q \sim 1(\sigma^{-1})$) the generally quadratic form of the Kratky plot arising from point particle (i, i) scattering is modulated by an oscillation attributable to adjacent segment ($i, i+1$) scattering. Over this range ($1 < Q < 32(\sigma^{-1})$) the IC and MC data are graphically indistinguishable. Only the region relating to the macromolecular geometry ($0 < Q < 1(\sigma^{-1})$) is presented here although the entire function is, of course, required for the transformations involved in the determination of the real-space configurational quantities. The agreement is seen to be good over the entire range of the scattering function. The IC determination appears to be a substantial improvement upon both the Debye estimate (eq 7) and the Nagai moment expansion (eq 8) which we have determined up to the 22nd moment on the basis of the Monte Carlo data. Previous authors have noted the very slow oscillatory convergence of this series,^{7,9} and we question whether the apparently good description of the oscillatory scattering function of s-PMMA reported by Yoon and Flory⁵ is not simply an artifact of the Nagai polynomial of degree n trying to have n roots. Such an artifact is apparent in Figure 2 based on Nagai moments $m \leq 22$.

Also presented is the persistence chain result, for although it totally neglects excluded volume, this model does incorporate the effects of restrictions on the valence angle between successive bonds. And although we refer to the present unit hard-sphere sequence as being "perfectly flexible", the valence angle is nevertheless geometrically restricted to the range $0-120^\circ$. In the absence of further chain interference a mean valence angle $\langle \alpha \rangle = 60^\circ$ is adopted, yielding $b = 3$ in eq 9, and the resulting curve

Table I
Weighting Functions W_ν for Scattering from Centers $i, i+\nu$ within the N -mer

	W_0	W_1	W_ν
linear	N	$2(N-1)$	$2(N-\nu)$
ladder	N	$5N-8$	$4N-8\nu$
ring	N	$2N$	$2N (W_{N/2} = N)$
star	$N =$ $nf+1$	$2nf =$ $2(N-1)$	$2f(n-\nu+1) + f(f-1)(\nu-1),$ $\nu \leq n; f(2n-\nu+1)(f-1), \nu > n$

is included in Figure 2. It is quite clear that the IC technique yields the closest description yet of the scattering function, judged on the basis of the Monte Carlo estimates. We note that the MC Kratky plot maintains a positive slope at intermediate Q , consistent with eq 18 and attributed to excluded-volume processes on the scale of several segment diameters. The MC curves show a systematic tendency toward a plateau region characteristic of unperturbed systems at intermediate Q with increasing chain length. As Yoon and Flory⁵ point out, however, it does not follow that this is an indicator of effectively unperturbed behavior but rather that approximate agreement with Debye behavior should be regarded as fortuitous compensation of departures from assumption (i) by corresponding departures from assumption (ii) (see above). Other authors² have shown that apparent Debye-like behavior may be produced by choosing appropriate ratios of the contrast factors $g_i g_j$. The IC determinations appear to achieve such a form at shorter chain lengths; this is an artifact of the approximation which we attribute to a degree of segment interpenetration inherent in the IC technique. It is significant that the IC and MC curves coincide almost exactly in all but the intermediate range of Q , where the agreement is nevertheless substantially better than for the three other approximations, which we now consider.

The Debye curve (eq 7) characteristic of small Q scattering from Gaussian chains clearly affords a poor representation of the MC data: the height of the plateau region substantially overestimates the chain flexibility, as might be expected from an unperturbed sequence. Estimates based on the Nagai series for $\langle \sin Qr_{ij}/Qr_{ij} \rangle$ (eq 8) are also shown in Figure 2. Curves incorporating terms up to and including the 6th, 12th, and 22nd moment of all intersegmental separations were determined in the course of the MC simulations. It is clear that convergence is slow, to say the least, and the curves appear to contain considerable structure which may or may not be spurious. Finally, the persistence chain result based on eq 10 is shown with the parameter $b = 3$. As discussed above, this corresponds to a mean valence angle $\langle \alpha \rangle = 60^\circ$, which would appear appropriate for the flexible hard-sphere sequences considered here. Certainly the resulting curve is a substantial improvement upon the Debye representation, but nevertheless remains in poor agreement with the MC data.

In Figure 3 we show the total and some of the principal components of the Kratky plot for a linear hard-sphere sequence of 20 segments determined on the basis of the IC approximation. Clearly, the scattering from the 20 point centers (the i, i terms in eq 4) dominates the Kratky plot, particularly at intermediate to large values of the scattering vector. Generally, for linear sequences, there will be $2(N-\nu)$ contributions arising from scattering between segments $(i, i+\nu)$ separated by ν links within the N -mer (Table I). Thus, the oscillation of the total curve in Figure 3 about the quadratic point scattering component (i, i) is primarily attributable to the $W_1 = 38$ adjacent-center ($i, i+1$) components. The subsequent components, each arising with weighting $2(N-\nu)$, represent the contribution to the total scattering from progressively longer

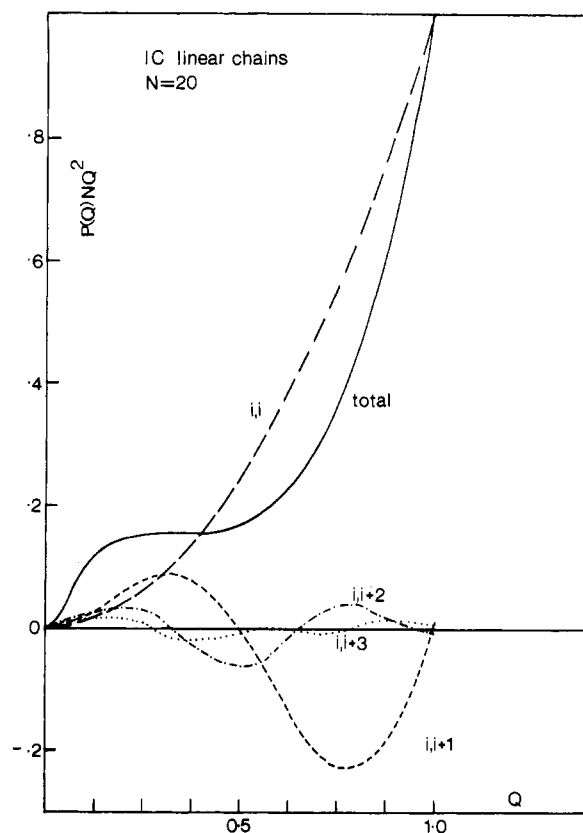


Figure 3. Total and principal components of the Kratky plot for a linear hard-sphere sequence ($N = 20$) determined in the IC approximation. Total curve (—); 20 (i, i) (—); 38 ($i, i+1$) (---); 36 ($i, i+2$) (···); 34 ($i, i+3$) (— · —).

subsets $0 < \nu < N$ within the sequence. (Of course, the $2(N-\nu)$ contributions to the ν -segment scattering within the N -mer will not be identical since the geometrical properties of the subset will depend upon its location within the sequence.) A number of important features should be noted. First, all component contributions $\nu \geq 1$ are oscillatory and, in particular, at small Q are all positive monotonically increasing functions of the scattering vector. This implies that *all* subsets ν contribute without self-cancellation to the Guinier region of the curve, as indeed they should since this relates directly to the radius of gyration of the sequence (eq 6). At intermediate values of Q , however, the tendency toward a plateau in the Kratky plot is clearly attributable to cancellation among oscillatory components arising from short to intermediate subset scattering, and in no way is Gaussian behavior implied over these spatial ranges. Thus, the assertion of Yoon and Flory that any tendency toward plateau form should be attributed to cancellation of assumptions (i) and (ii) above appears substantiated.

Ladder polymers represent a related class of linear sequences for which IC determinations of the configurational and scattering properties may be readily determined. Basically, such systems consist of two identical linear hard-sphere sequences of the type described above, each of length $N/2$, but with an additional sequential connection between the two chains, i.e., $1-1', \dots, i-i', \dots, N/2-N/2'$ where ' distinguishes between the two linear parallel sequences. There will now be in addition substantial interchain scattering from contiguous segments separated by the hard-sphere collision diameter (Table I), and this is clearly apparent from the Kratky plots shown in Figure 4. While sequential connectivity in simple linear sequences ensures that scattering arises from adjacent segments, the interchain contribution produces a strong os-

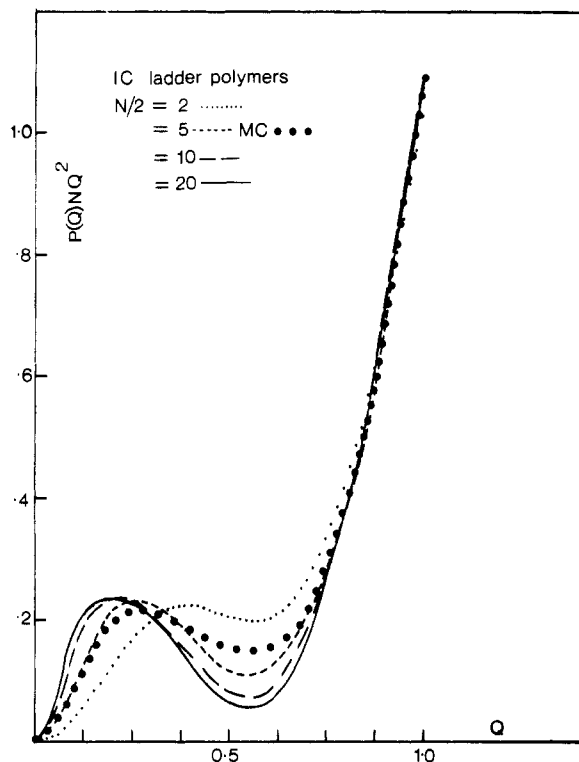


Figure 4. Kratky plots for perfectly flexible linear hard-sphere ladder sequences on the basis of the IC approximation. Also shown is the corresponding Monte Carlo result for $N/2 = 5$.

cillation in the curve which develops in amplitude with increasing N , while the maximum shifts systematically with chain length to smaller Q as scattering on progressively larger inter- and intrachain spatial scales develops. Obviously the $2((N/2) - 1)$ strongly oscillatory $(i, i+1)$ contributions arising from the two parallel linear chains will be supplemented by a further $N/2$ (i, i') terms of identical form arising from the "rungs" of the ladder. This will be further enhanced by a very similar component of weight $2((N/2) - 2)$ arising from $(i, i'+1)$ scattering. It is clear from Table I that this scattering component will be substantially stronger than for its linear counterpart of identical molecular weight. As we have seen in Figure 3, these scattering contributions are responsible for the strong oscillation in the Kratky curve, and immediately account for the form of scattering in ladder polymers. It appears that little consideration of the structural and scattering properties of such systems has appeared in the literature as yet. A Monte Carlo analysis of ladder polymers of $N/2 = 5$ is also shown in Figure 4, and this is seen to be in reasonable agreement with the IC determination.

One further consequence of the enhanced $(i, i+1)$ scattering arising in ladder polymer systems is the increased oscillation about the quadratic (i, i) scattering over the range $Q \geq 1(\sigma^{-1})$. In fact, this development was confirmed over the range $1 < Q < 32(\sigma^{-1})$ for both the IC and MC analyses, which again were found to be graphically indistinguishable.

Ring Polymers

Equation 15, based on Gaussian rings, predicts a maximum in the Kratky plot attributable to short-range effects, followed by the usual Debye plateau at larger Q . The IC calculations also predict a weak maximum for smaller rings (Figure 5) which gradually disappears with increasing ring size, followed in all cases by a strong rise at large Q reflecting the departure from Gaussian statistics over short spatial ranges assumed to hold in eq 7 and 15. In fact, the

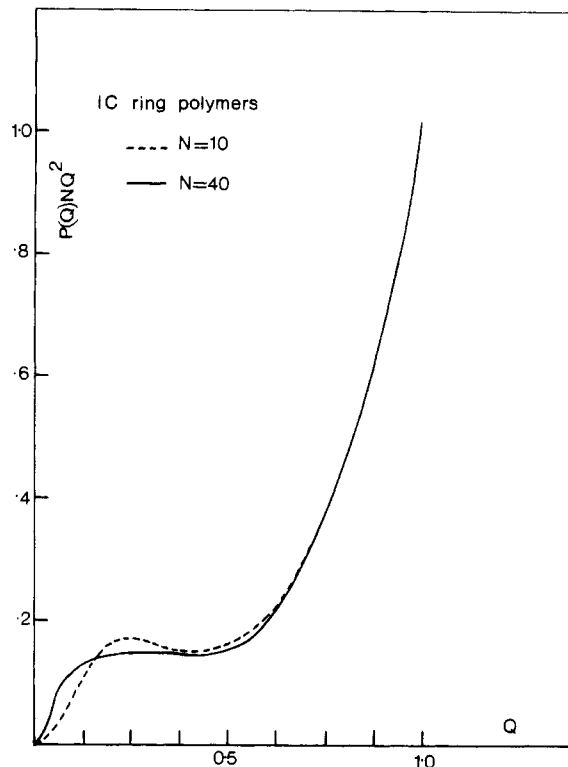


Figure 5. Kratky plots for perfectly flexible hard-sphere rings determined on the basis of the IC approximation.

difference between scattering from a ring and a linear sequence arises from the weighting factor: scattering from segments $(i, i+\nu)$ assumes a weighting factor of $2(N - \nu)$ for linear sequences while for rings the weighting is $2N$ (except $W_{N/2} = N$) (Table I), regardless of the value of ν . Thus, the principal contributions to ring scattering are very similar to those from linear sequences of the same molecular weight, particularly when $N \gg n$. Thus, the Kratky curves for rings and linear chains are very similar and appear not to show the weak maximum predicted by eq 15, except for the smallest rings considered here. Similar behavior has been reported for scattering from cyclic poly(dimethylsiloxane) (PDMS)¹⁷ on the basis of Monte Carlo RISM calculations. In fact, a double maximum in the Kratky plots was observed by these authors for $N < 40$ skeletal bonds, the structure maximizing in the vicinity of $N = 22$. This, however, was considered to be a feature peculiar to the PDMS ring molecule which is known to form a low energy all-trans planar loop at $N = 22$ and cannot be attributed to $(i, i+1)$ scattering, although this strong oscillatory component will extend to large values of the scattering vector. Similar calculations for short polymethylene (PM) rings also revealed a double maximum, though without any particular enhancement at specific N . These features are undoubtedly associated with the specific skeletal geometry assumed for the PDMS and PM systems in the RISM calculations (which, incidentally, neglect excluded-volume effects) since the second maximum disappears with increasing ring size and flexibility of the molecule. In fact, there appears good qualitative agreement between the RISM calculations for large rings (when the details of the skeletal geometry are suffused) and the present IC determinations. The above authors¹⁷ report reasonable agreement between their RISM calculations and SANS experiments on PDMS, at least at small Q , while the semi-Gaussian approximation (eq 15) of Cassassa and Burchard and Schmidt¹² appears to provide a poor description of ring scattering at all but the smallest Q , even on a qualitative basis.

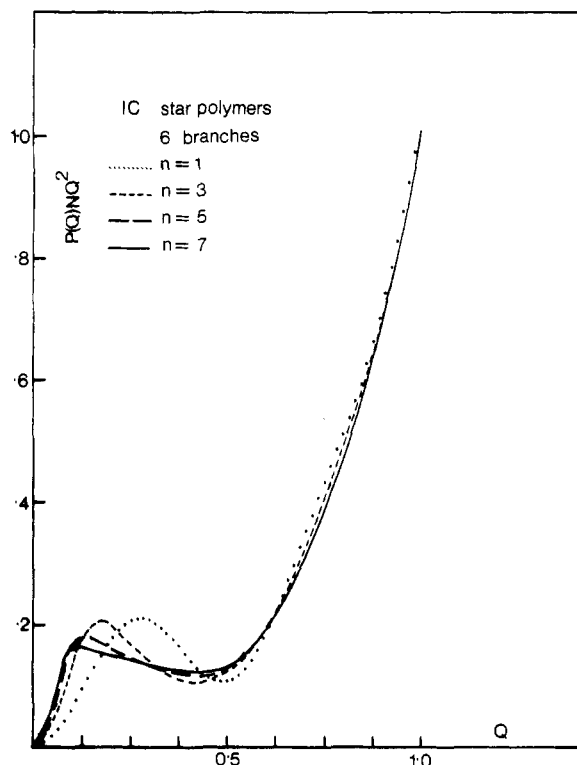


Figure 6. Kratky plots for perfectly flexible uniform hard-sphere stars of $f = 6$ branches having $n \leq 7$ monomers per branch, determined in the IC approximation. Also shown is the corresponding Monte Carlo estimate.

Star Polymers

We have previously reported the configurational properties of perfectly flexible hard-sphere uniform star polymers determined in the IC approximation.¹⁹ Although passing mention was made to the scattering properties of such systems, that paper was primarily concerned with the resolution of the Daoud-Cotton hypothesis¹⁸ of distinct interior configurational regimes within the star and the scaling properties of the system with molecular weight, N . Gaussian expressions for the scattering function, largely restricted to the Guinier region, are available (eq 14), but these do not, of course, address the basic problem of perturbed systems over the entire scattering range. In Figure 6 we show the Kratky plots for $f = 6$ branch uniform hard-sphere stars having $n \leq 7$ monomers per branch, determined in the IC approximation. In all cases the Kratky function shows a pronounced oscillation, damping out with increasing branch length at given functionality, f . This behavior was confirmed on the basis of Monte Carlo simulations¹⁹ and differs substantially from the Debye function predicted on the basis of eq 14. Such behavior may be readily understood on the basis of the weighting factors presented in Table I. We note that with increasing molecular weight the scattering becomes more like that from a linear sequence, particularly at low functionality f . This is apparent from both the IC and MC determinations. However, the tendency to form a plateau region, as for linear sequences, does not imply Gaussian behavior over intermediate Q .

It is apparent from Figure 6 that the perturbed and unperturbed systems develop quite differently with increasing n at intermediate Q , although following the observations of Yoon and Flory,⁵ we stop short of identifying the tendency toward a plateau region in the perturbed systems with the onset of Gaussian behavior over intermediate spatial scales. As they point out, such apparent behavior can be largely fortuitous, reflecting only the

partial compensation of departures from one of the Gaussian assumptions (i.e., that $Z(ij|N)$ is Gaussian) by departures from the other ($\langle R_{ij}^2 \rangle \sim |i - j|$). Nevertheless, it should be said that Daoud and Cotton¹⁸ propose that at intermediate distances from the central vertex in a uniform self-avoiding star polymer the monomer concentration is likely to exhibit a Gaussian behavior, and presumably scattering from these regions would make contributions of the Debye type. It is possible to interpret the Kratky plots at intermediate Q in this sense, however, detailed Monte Carlo and IC determinations¹⁹ suggest this is not the case and the caution expressed by Yoon and Flory in drawing such conclusions again seems appropriate.

Conclusions

The iterative convolution technique, previously used for the description of a wide variety of real-space geometrical properties of finite self-interacting polymer sequences, has been extended to the prediction of the molecular scattering function $P(Q)$, generally presented in the form of a Kratky plot. Although calculations so far have generally been restricted to perfectly flexible hard-sphere systems, the technique readily extends to more realistic, and indeed, heterogeneous interactions, both in the presence and absence of a surrounding solvent. The description of hard-sphere systems as a caricature of the excluded-volume feature has generally been a necessary precursor in the statistical mechanical description of realistic systems, and it is in that sense that we have been primarily occupied with hard-sphere representations here. Given that there is no corresponding body of experimental data, the hard-sphere interaction proves to be particularly convenient for the purposes of Monte Carlo simulation, and we complement our IC determinations with MC simulations wherever possible.

For all polymer geometries investigated in this paper, previous predictions of the scattering function were generally restricted to small Q or asymptotic representations, almost invariably based on Gaussian statistics, or perturbative departures therefrom, and in no case were they able to describe the full range of scattering vector Q . The Debye model, while able to provide a reasonable description in the very small Q Guinier region of scattering, rapidly became inappropriate over ranges of Q appropriate to spatial scales similar to the correlation length between monomers within the system. The Nagai series expansion of $\langle \sin Qr_{ij} \rangle / \langle Qr_{ij} \rangle$ arising in the definition of the scattering function proved to show an extremely slow, oscillatory convergence toward the correct scattering function, even when based upon exact Monte Carlo data as input. There is, moreover, some suspicion that the structural features observed in the Nagai representation are in fact spurious, being artifacts of an n -th term polynomial. The persistence chain model permits a unified description of linear Gaussian through rigid-rod systems in terms of a stiffness parameter: excluded-volume processes do not feature in this representation, and accordingly the model affords a poor description of the flexible hard-sphere systems described here.

In each case the IC technique yields excluded-volume Kratky functions in good to excellent agreement with their Monte Carlo counterparts over the entire range of scattering function Q and for a wide variety of polymer geometries including linear polymers, ladder polymers, rings, and stars. A number of distinctive features of the scattering function for specific molecular geometries are identified and interpreted and in all cases confirmed by the Monte Carlo simulations. We conclude that the IC technique, for flexible hard-sphere systems at least, ap-

pears to provide a unified description of real-space configurational structures and their corresponding scattering functions for a wide variety of finite polymer systems in generally good agreement with simulated data.

The component scattering arising from centers $i, i+\nu$ is readily determined by means of the IC technique, and in conjunction with the associated weighting functions W_ν (Table I) provides a unified approach to the structure of the Kratky plot, regardless of polymer structure for systems of identical molecular weight. The W_0 factors are obviously independent of the molecular structure; the W_1 , however, are already sensitive to the molecular geometry and appear responsible for the characteristic oscillation in ladder and star scattering functions. In all cases the components are oscillatory and there appears no evidence of the Gaussian transforms presumed responsible for the Debye plateau. This does not preclude the development of a plateau region in the scattering curve, but its appearance cannot be attributed to Gaussian behavior within the system.

Acknowledgment. I thank Ruby Turner for the numerical computations, Dr. Paul Barnes for helpful discussions, and ARGS for financial support.

References and Notes

- (1) Kirste, R. L.; Oberthur, R. L. In *Small-Angle X-ray Scattering*; Glatter, O., Kratky, O., Eds.; Academic: London, 1982; Chapter 12.
- (2) Edwards, C. J. C.; Richards, R. W.; Stepto, R. F. T. *Macromolecules* 1984, 17, 2147.
- (3) Heine, S.; Kratky, O.; Roppert, J. *Makromol. Chem.* 1962, 56, 150. Yoon, D. Y.; Flory, P. J. *J. Chem. Phys.* 1978, 69, 2537. Hayashi, H.; Flory, P. J.; Wignall, G. D. *Macromolecules* 1983, 16, 1328.
- (4) Debye, P. *J. Phys. Chem.* 1947, 51, 18.
- (5) Flory, P. J.; Jernigan, R. L. *J. Am. Chem. Soc.* 1968, 90, 3128. Yoon, D. Y.; Flory, P. J. *Macromolecules* 1976, 9, 294. *Ibid* 1976, 9, 299.
- (6) Mattice, W. L.; Santiago, G. *Macromolecules* 1980, 13, 1560. Mattice, W. L. *Macromolecules* 1982, 15, 18. Mattice, W. L. *Macromolecules* 1982, 15, 579.
- (7) Zierenberg, B.; Carpenter, D. K.; Hsieh, J. H. *J. Polym. Sci., Polym. Symp.* 1976, 54, 145.
- (8) Flory, P. J. *Statistical Mechanics of Chain Molecules*; Interscience: New York, 1969.
- (9) Mattice, W. L.; Carpenter, D. K. *J. Chem. Phys.* 1976, 64, 3261.
- (10) Neugebauer, T. *Ann. Phys. (Leipzig)* 1943, 42, 509.
- (11) Benoit, H. *J. Polym. Sci.* 1953, 11, 507.
- (12) Casassa, E. F. *J. Polym. Sci. Part A* 1965, A3, 605. Burchard, W.; Schmidt, M. *Polymer* 1980, 21, 745.
- (13) Zimm, B. H.; Stockmayer, W. H. *J. Chem. Phys.* 1949, 17, 1301.
- (14) des Cloiseaux, J. *Macromolecules* 1973, 6, 403.
- (15) Fisher, M. E. *J. Chem. Phys.* 1966, 44, 616.
- (16) Abramowitz, M.; Stegun, I. *A Handbook of Mathematical Functions*; Dover: New York, 1970.
- (17) Edwards, C. J. C.; Richards, R. W.; Stepto, R. F. T.; Dodgson, K.; Higgins, J. S.; Semlyen, J. A. *Polymer* 1984, 25, 365.
- (18) Daoud, M.; Cotton, J. P. *J. Phys. (Les Ulis, Fr.)* 1982, 43, 531.
- (19) Croxton, C. A. *Macromolecules* 1988, 21, 2269.
- (20) Croxton, C. A. *Macromolecules*, in press, and references contained therein.
- (21) Croxton, C. A. *J. Phys. A: Math. Gen.* 1984, 17, 2129.
- (22) Yamakawa, H. *Modern Theory of Polymer Solutions*; Harper and Row: New York, 1971; pp 12-18.
- (23) Sharp, P.; Bloomfield, V. A. *Biopolymers* 1968, 6, 1201.

Intercomparisons of Dielectric Relaxation, Dynamic Light Scattering, and Viscoelastic Properties of the Local Segmental Motion in Amorphous Polymers

K. L. Ngai*

Naval Research Laboratory, Washington, D.C. 20375-5000

S. Mashimo

Department of Physics, Tokai University, Hiratsuka-shi, Kanagawa 259-12, Japan

G. Fytas

Department of Chemistry, University of Crete, Iraklion, Crete, Greece.

Received November 30, 1987; Revised Manuscript Received February 22, 1988

ABSTRACT: Independent of the nature of the probe (e.g., longitudinal compliance by dynamic light scattering, shear compliance by dynamical compliance and modulus or by creep recovery, electric compliance by dielectric relaxation) near and above the glass temperature, the appropriate correlation or relaxation function of the local segmental motion in an amorphous polymer is well described by the Kohlrausch-Williams-Watts function $\exp\{-(t/\tau^*)^{1-n}\}$. The temperature dependence of the effective time τ^* is well represented by the Vogel-Fulcher-Tamann-Hesse equation $\tau^* \propto \exp\{B/(T - T_0)\}$. However, the fractional exponent n and the quantity B , for a fixed T_0 , can depend on the nature of the probe. Through a compilation of the experimental data of a number of amorphous polymers, we have established an empirical correlation between n and B . Whenever the two quantities n and B are probe dependent in an amorphous polymer, we find the product $(1 - n)B$ remains invariant. An explanation of this empirical relation can be found from an extant prediction of the coupling model of relaxation.

Introduction

It has been noticed repeatedly¹⁻¹¹ in the course of the study of local segmental motion (i.e., relaxation of small portions of backbone chain that is responsible for volume and enthalpy recovery near the glass temperature T_g often referred to as the α relaxation) in polymers that there can

be a significant difference between its relaxation time determined dielectrically and its relaxation time obtained from either photon correlation spectroscopy or viscoelastic (mechanical) measurement. The same is true for non-polymeric glass-forming liquids such as *o*-terphenyl.¹² Examples in polymers include poly(propylene glycol)¹